

Time-dependent local-density theory of dielectric effects in small molecules

Zachary H. Levine* and Paul Soven

Department of Physics and Laboratory for Research on the Structure of Matter, University of Pennsylvania, Philadelphia, Pennsylvania 19104

(Received 15 August 1983)

A time-dependent local-density theory of the photoemission spectra and polarizabilities of finite systems is extended from atoms to molecules. The theory is implemented in a single-center formulation and is applied to N_2 and C_2H_2 . The partial photoemission cross sections and asymmetry parameters for the $1\pi_g$ and $3\sigma_g$ levels are presented as well as the optical-frequency polarizabilities; agreement with experiment is generally, but not uniformly, excellent.

I. INTRODUCTION

It has long been known that dynamical internal screening (which we denote as "dielectric" effects) significantly affects the static and dynamical response of atoms, molecules, and solids to an externally applied electromagnetic field. In comparison with independent-particle calculations, one finds that for low-frequency fields there is a considerable reduction in the magnitude of both the linear polarizability¹⁻⁴ $\alpha(\omega)$ as well as the hyperpolarizability.⁵ At higher frequencies (as probed, for example, by the photoemission cross section) the collective effects responsible for the dielectric screening characteristically shift oscillator strength to higher frequencies and broaden and shift spurious peaks predicted by an independent-particle calculation.¹ This same mechanism can act on a discrete transition to produce a large contribution to the photoemission cross section where none existed before.^{6,7} Since the Augerlike decay of excited particle-hole pairs are an essential part of the dielectric response treatment, autoionization resonances resulting from a discrete state mixing with the (degenerate) continuum states⁸ arise in this theory in a completely natural way.^{4,9} In a fair proportion of the cases studied to date, dielectric effects are sufficiently large to produce qualitative as well as quantitative effects in the photoemission spectrum.

The motivation for including dielectric effects in the study of the electronic properties of finite systems is clear. Following Zangwill and Soven,^{1,4} we believe that the most practical way to do this is with a self-consistent time-dependent perturbation theory based on a local-density-functional approximation to the ground state of the system. This approximation is known as the time-dependent local-density approximation, or TDLDA. Formally the procedure is similar to conventional time-dependent Hartree (random-phase approximation) and time-dependent Hartree-Fock (random-phase approximation with exchange).¹⁰⁻¹² It differs in the use of a local potential to treat exchange and correlation. Experience with the atomic system suggests that basing the theory on the local-density ground state, rather than the Hartree-Fock ground state, leads to much more accurate results with only a fraction of the computational effort.

The theory^{1,4} is quite straightforward. The external field acting on the system is described by a scalar potential $\varphi^{\text{ext}}(\vec{r}, \omega)$. (Retardation effects, which require a full vector-potential description of the electromagnetic field, are unimportant for systems of atomic or molecular dimensions.) In the independent-particle approximation (IPA) the particle density $\delta n(\vec{r}, \omega)$ induced by this field is given by the expression

$$\delta n(\vec{r}, \omega) = \int \chi_0(\vec{r}, \vec{r}', \omega) \varphi^{\text{ext}}(\vec{r}', \omega) d^3\vec{r}',$$

where $\chi_0(\vec{r}, \vec{r}', \omega)$ is the (exact) independent-particle density-density response function. We account for internal screening of this field by recognizing that the induced charge density gives rise to an induced field equal to the sum of a Coulomb potential (which a classical external test charge would experience in the vicinity of the system) and an induced exchange-correlation field. Thus, a more nearly correct expression for the induced charge is

$$\delta n(\vec{r}, \omega) = \int \chi_0(\vec{r}, \vec{r}', \omega) \varphi^{\text{SCF}}(\vec{r}', \omega) d^3\vec{r}', \quad (1)$$

where $\varphi^{\text{SCF}}(\vec{r}, \omega)$ is the sum of the external field and the two induced fields just described.

The Coulomb potential is

$$\delta V_C(\vec{r}, \omega) = e^2 \int \frac{\delta n(\vec{r}', \omega)}{|\vec{r} - \vec{r}'|} d^3\vec{r}', \quad (2)$$

where e is the charge on an electron. We compute the induced exchange-correlation potential by linearizing the local-density-functional exchange-correlation potential $V_{\text{xc}}(\vec{r})$ about the ground-state value:

$$\delta V_{\text{xc}}(\vec{r}, \omega) = \frac{\partial V_{\text{xc}}(\vec{r})}{\partial n} \delta n(\vec{r}, \omega). \quad (3)$$

The TDLDA consists of solving Eqs. (1)–(3) simultaneously. An essential simplifying feature, compared to time-dependent Hartree-Fock theory, is that the properties of the unperturbed system enter only through the density-density response function which in turn may be calculated

in terms of Green's functions, avoiding the complication of infinite summations over virtual states. The independent-particle susceptibility is given by the expression

$$\chi_0(\vec{r}, \vec{r}', \omega) = \sum_i^{\text{occ}} \psi_i^*(\vec{r}) \psi_i(\vec{r}') \sum_j \frac{\psi_j(\vec{r}) \psi_j^*(\vec{r}')}{\epsilon_i - \epsilon_j + \hbar\omega + i\eta} + \sum_i^{\text{occ}} \psi_i(\vec{r}) \psi_i^*(\vec{r}') \sum_j \frac{\psi_j^*(\vec{r}) \psi_j(\vec{r}')}{\epsilon_i - \epsilon_j - \hbar\omega - i\eta},$$

where the sum on i runs over all occupied single-particle states, and the sum on j runs over all single-particle states; ϵ_i is an eigenvalue, $\hbar\omega$ is the photon energy, and η is an infinitesimal. Transitions from occupied to occupied states cancel between the two terms, so their inclusion is a matter of convenience. The spectral representation of the response function allows it to be expressed in terms of the single-particle Green's function of the system,

$$\chi_0(\vec{r}, \vec{r}', \omega) = \sum_i^{\text{occ}} \psi_i^*(\vec{r}) \psi_i(\vec{r}') G(\vec{r}, \vec{r}', \epsilon_i + \hbar\omega) + \sum_i^{\text{occ}} \psi_i(\vec{r}) \psi_i^*(\vec{r}') G^*(\vec{r}, \vec{r}', \epsilon_i - \hbar\omega),$$

where

$$G(\vec{r}, \vec{r}', E) = \sum_j \frac{\psi_j(\vec{r}) \psi_j^*(\vec{r}')}{E - \epsilon_j + i\eta}. \quad (4)$$

Since the ground-state potential is local, the Green's function satisfies the differential equation

$$[E + \nabla^2 - V(\vec{r})]G(\vec{r}, \vec{r}', E) = \delta(\vec{r} - \vec{r}') \quad (5)$$

in both the \vec{r} and \vec{r}' variables. Owing to the particularly simple nature of the inhomogeneous term in Eq. (5), the solution is only slightly more difficult than determining the solution of the related homogeneous equation in a single spacial variable. The sign of the infinitesimal determines the boundary conditions on the Green's function at infinity. Since the TDLDA is a self-consistent first-order perturbation theory about the local-density-functional (LDF) ground state, the potential in (5) corresponds to a neutral system and does not contain a long-range Coulomb component.

All observable quantities may be computed in terms of the frequency-dependent self-consistent charge density and potential. Any component $\alpha_\nu(\omega)$ of the polarizability tensor (diagonal in the cases of interest) is proportional to the induced dipole moment

$$\alpha_\nu(\omega) = e^2 \int x_\nu \delta n(\vec{r}', \omega) d^3 \vec{r}',$$

in unit external field oriented in the corresponding direction. The total photoemission cross section (for the electric field in the ν th direction) is proportional to the imaginary part of the polarizability

$$\sigma_\nu(\omega) = -4\pi\alpha\hbar\omega \text{Im} \int x_\nu \delta n(\vec{r}', \omega) d^3 \vec{r}',$$

where α is the fine-structure constant. Partial photoemission cross sections are related to the probability of leaving

the ion in a particular final state. The conventional "golden-rule" expression may be employed, with the substitution of the self-consistent field for the external one. Thus

$$\sigma_{i\nu}(\omega) = \alpha\hbar\omega E_f^{1/2} |\langle \psi_i | \varphi_\nu^{\text{SCF}}(\vec{r}, \omega) | \psi_f \rangle|^2, \quad (6)$$

where it is assumed that the final states are scaled asymptotically to plane waves and E_f is final-state energy. The sum of the partial cross sections is the total cross section under these definitions, so long as $\varphi^{\text{SCF}}(\vec{r}, \omega)$ is indeed a self-consistent field as defined above. The independent-particle approximation arises by using $\varphi^{\text{ext}}(\vec{r}, \omega)$ instead of $\varphi^{\text{SCF}}(\vec{r}, \omega)$ in Eqs. (1) and (6).

In addition to the total cross section, photoemission experiments give some information about the angular distribution of the outgoing photoelectrons. For a gas-phase target consisting of randomly oriented nonchiral molecules, in the electric dipole approximation the photoemission angular distribution is given by¹³

$$\frac{d\sigma}{d\Omega}(\omega) = \frac{\sigma(\omega)}{4\pi} [1 + \beta(\omega) P_2(\cos\vartheta)]$$

where ϑ is the angle between the electric field (of a linearly polarized electromagnetic wave) and the outgoing electron direction, and $\beta(\omega)$ is the photoemission asymmetry parameter. A formula for β in terms of partial-wave matrix elements $I_{lm\nu}$ is well known,¹⁴

$$\beta = \frac{3}{5S} \sum_{\substack{l, m, \nu \\ l', m', \nu'}} I_{lm\nu} I_{l'm'\nu'}^* (-1)^{\nu' - m'} \times C(11200)C(112\nu - \nu')C(l'l'200) \times C(l'l'2m - m'), \quad (7)$$

where

$$S = \sum_{L, \nu} |I_{L\nu}|^2$$

and the C 's are Clebsch-Gordan coefficients. The partial-wave matrix elements are given by

$$I_{L\nu} = \langle \psi_i | \varphi_\nu | \psi_f^{(L)} \rangle$$

where the final state is an integral transform of the usual plane-wave-plus-incoming-spherical-wave final states $\psi_{\vec{k}}(\vec{r})$

$$\psi_f^{(L)}(\vec{r}) = \int \psi_{\vec{k}}(\vec{r}) Y_L(\Omega) d\Omega.$$

Use of the self-consistent field in place of the external field does not effect the validity of the above formulas, even though the self-consistent field is far from uniform in space. The induced field is a linear function of the external field; as such it has the same (vector) transformation properties which underlie the formula for β .

The theory just described has already been used to study the polarizability¹⁻⁴ and photoemission cross section^{1,4,7}

of atoms and the hyperpolarizability of rare-gas atoms.⁵ In general, the theory was successful at the level of a few percent, in contrast to the independent-particle approximation which was not even qualitatively correct in a number of cases. Results are generally at least as good as those obtained with other approximations. In view of these successes, we felt that it would be desirable to extend the theory from atoms to small molecules. It is the purpose of this paper to describe the formalism we used to make this extension, and to present the results obtained in the cases of molecular nitrogen and acetylene. A letter presenting some of the acetylene results has already appeared.⁹ A recent article reviews the field of molecular photoionization as a whole.¹⁵

II. MOLECULAR SINGLE-CENTER FORMULATION

Implementation of the theory just described requires knowledge of the bound states and the Green's functions in a given geometry. The description of these quantities must be sufficiently simple that the fundamental equations of the theory may be solved. We have chosen to represent both the eigenfunctions and the Green's function using a single-center expansion about the molecular center. This representation provides a conceptual and, more importantly, computational simplicity in finding the induced potential, which, however, is somewhat counterbalanced by the (notorious) difficulty of solving molecular problems with a single-center representation.

Our strategy for circumventing some of the difficulties of the single-center expansion was to complete the *ground-state* calculation in a Gaussian basis representation and then project needed quantities onto a single-center spherical harmonic representation. We performed a self-consistent-field calculation in the local-density approximation,^{16,17} using the Gaussian-orbital program developed by Dunlop, Connolly, and Sabin.¹⁸ Basis sets consisting of 11s, 6p, and 3d orbitals on the nitrogen or carbon atoms, 7s and 2p orbitals on each hydrogen, and two diffuse s orbitals at the molecular center were used. These basis sets are slight extensions of those suggested by van Duijneveldt.¹⁹ We chose the average atomic Schwarz²⁰ values for the $X\alpha$ parameter, namely 0.751 97 for nitrogen and 0.768 26 for acetylene. The potential was found self-consistently in the Gaussian-orbital basis, projected into the single center, and used without further modification. The bound-state wave functions were recomputed in the single center, as indicated below. Valence eigenvalues calculated using the single-center expansion differed by about 1 eV from the Gaussian-orbital predictions when all symmetry allowed spherical harmonics up to $l=19$ were included. The exchange-correlation potential taken from the Gaussian-orbital program was used to derive the value of $\partial V_{xc}(\vec{r})/\partial n$. We used the $X\alpha$ approximation, rather than the more nearly correct density functionals¹⁷ employed in the work of Zangwill and Soven;^{1,4,5,7} however, only minor changes result from this replacement.

In the single-center expansion a solution $\psi(\vec{r})$ to the coupled-channel equations is expanded in the form

$$\psi(\vec{r}) = \sum_L \psi_L(r) Y_L(\Omega),$$

where the $\psi_L(r)$ form the solution vector of $\psi(\vec{r})$, Y_L is a spherical harmonic, and L is a compact representation of the two angular momentum indices l and m . If the expansion is terminated after a finite number of terms and the variational principle is applied, we arrive at the coupled-channel Schrödinger equation

$$\sum_{L'} [(\nabla_L^2 + E)\delta_{LL'} - V_{LL'}(r)] \psi_{L'}(r) = 0, \quad (8)$$

where

$$\nabla_L^2 = \frac{1}{r} \frac{d^2}{dr^2} r - \frac{l(l+1)}{r^2}.$$

The quantities $V_{LL'}$ are related to the physical potential by the transformation

$$V_{LL'}(r) = \sum_{L''} C_{LL'L''} \int V(\vec{r}') Y_{L''}(\Omega) d\Omega, \quad (9)$$

where the $C_{LL'L''}$ are the Gaunt integrals $\int Y_L Y_{L'} Y_{L''}^* d\Omega$. Symmetry may be included by allowing only some of the spherical harmonics in the sum. (A trivial generalization is needed for, e.g., cubic harmonics.) Given an external potential, we find a bound state using the method of Gordon.²¹ For a given energy there are a set of $2N$ solutions to the system of N second-order differential equations (8), where N denotes the number of symmetry allowed (l, m) components within the truncated angular momentum subspace. Of these N are regular at the origin (the inner solutions), and N vanish exponentially at infinity for negative energies (the outer solutions). A bound state exists for those discrete energies for which some linear combination of the N inner solutions is equal in slope and value to some linear combination of the N outer solutions. We found that the nucleus of the heaviest element was the best place to match the inner and outer solutions, because the components of the solution vectors with large L are big only in this region. By finding the energy of solution to great precision (a part in 10^{12}), even the smallest components of the solution vector could be made to join smoothly from the inner to the outer solutions.

The Green's function may be expanded in the single-center form

$$G(\vec{r}, \vec{r}', E) = \sum_{L, L'} Y_L(\Omega) G_{LL'}(r, r', E) Y_{L'}(\Omega'),$$

where the components $G_{LL'}$ satisfy the coupled equations

$$\sum_{L''} [(\nabla_L^2 + E)\delta_{LL''} - V_{LL''}(r)] G_{L''L'}(r, r', E) = \frac{\delta_{LL'} \delta(r - r')}{rr'} \quad (10)$$

in both radial variables. The angular momentum decomposition of the Green's function is a crucial quantity in our theory. We have found a convenient representation of this quantity in terms of the regular and irregular eigenchannel^{14,22} solutions of the coupled-channel equations. The details of our constructive procedure are presented in the Appendix.

The self-consistent-field equations of the TDLDA are solved in a relatively straightforward manner. The in-

tegral to find the charge density (1), while nominally over space for each point in space, turns out to be no more difficult than doing a number of one-dimensional spacial integrations, thanks to the special form of G in Eqs. (A7) and (A8). The calculation of the Coulomb potential is simple because the integration kernel $|\vec{r}-\vec{r}'|^{-1}$ is diagonal in L when expanded in spherical harmonics. The exchange-correlation term involves only multiplication.

Self-consistency is achieved with a dual strategy: for several iterations (perhaps seven) the field resulting from going around the loop implied by Eqs. (1)–(3) is simply plugged back in to the charge-density integral (1). The error in the calculated $\varphi^{\text{SCF}}(\vec{r},\omega)$ may either grow or shrink (roughly geometrically) by this procedure. Then, the Aitken method of accelerated convergence²³ is applied to a three-term historical sequence of the components $\varphi_L^{\text{SCF}}(r)$, terms in the single-center expansion of $\varphi^{\text{SCF}}(\vec{r},\omega)$. Often a nearly self-consistent solution results from one Aitken step. Our convergence criterion was that $\varphi^{\text{SCF}}(\vec{r},\omega)$ reproduce itself to an absolute magnitude of 10^{-5} at all points in space, on a scale in which $\varphi^{\text{ext}}(\vec{r})=z$. Typically about ten iterations including perhaps two Aitken steps was sufficient to produce convergence.

With $\varphi^{\text{ext}}(\vec{r})=z$, the partial cross sections are given by

$$\sigma_{i,\nu}(\omega)=4\pi\alpha\hbar\omega\sum_n|\langle\psi_i|\varphi_\nu^{\text{SCF}}|\psi_n\rangle|^2,$$

where the eigenchannel continuum normalization of Eq. (A5) is required, rather than the plane-wave normalization of Eq. (6). Similarly, the partial-wave matrix elements needed to compute β in Eq. (7) are given in terms of the eigenchannels using the relation

$$I_{L,\nu}=\sum_n\langle\psi_i|\varphi_\nu^{\text{SCF}}|\psi_n\rangle e^{i\delta_n}U_{nL}i^l,$$

where ν is the light polarization index. These relationships may be derived by matching the asymptotic form of the eigenchannel solutions to the asymptotic form of a plane wave plus an incoming spherical wave, which is the final state in photoemission,²⁴ followed by an appropriate integration over angles.

III. RESULTS FOR NITROGEN AND ACETYLENE

A. General

Nitrogen and acetylene provide interesting model systems for a variety of reasons. There is a great deal of experimental data on both nitrogen^{25–34} and acetylene,^{33–39} as well as a number of theoretical calculations for nitrogen^{12,22,40–50} and acetylene.^{9,34,36,50,51} Despite considerable effort previous to this work, some of the data remains unexplained, or at least explained only qualitatively. The two molecules have filled shells in their ground states (unlike, for example, O_2), thus the problem of multiplets, which are difficult to describe in a local-density-functional theory, is avoided. Nitrogen and acetylene represent a favorable case numerically: They involve only first-row atoms which are combined into a high-symmetry configuration (namely $D_{\infty h}$). Even so, in calculating the photoemission partial cross sections, we found it necessary to restrict our attention to the molecular orbitals which are primarily derived from atomic p states, namely the $1\pi_u$ and the $3\sigma_g$. (The single-center expansion describes the nuclear regions least well; since the p -derived states have a node at or near the nuclei, they are the best described molecular wave functions.) Additionally, there is some virtue in studying nitrogen and acetylene together since they are isoelectronic.

Molecular nitrogen and acetylene each have 14 electrons. The occupied orbitals are the $1\sigma_g$ and the $1\sigma_u$, which are the atomic $1s$ levels; the $2\sigma_g$ and the $2\sigma_u$, bonding and antibonding combinations of functions with predominantly atomic $2s$ character; the $3\sigma_g$, which are bonding combinations of the atomic p_z levels (where the z direction is the molecular axis); and the orbitally degenerate $1\pi_u$, bonding combinations of atomic p_x and p_y levels. Additionally, our potential binds an unoccupied $1\pi_g$ level, the antibonding combination of p_x and p_y orbitals. All other bound states, such as the infinite collection of Rydberg states, are not present in the calculation because the ground-state potential is neutral.

The eigenvalues of our calculations, both in the Gaussian-orbital basis set and the single-center expansion, are shown in Table I. The two calculations are in agreement to within about 1 eV for the valence levels. To rationalize the eigenvalues, recall two simple facts: nitrogen

TABLE I. Eigenvalues and ionization potentials (IP) for nitrogen and acetylene (in eV).

Bound state	Nitrogen			Acetylene		
	Gaussian basis set	Single center	Expt. (Ref. 26) IP	Gaussian basis set	Single center	Expt. (Ref. 51) IP
$1\sigma_g$	–384.2	–346.0		–270.8	–247.5	
$1\sigma_u$	–384.1	–349.2		–270.8	–249.5	
$2\sigma_g$	–28.3	–27.5		–18.6	–17.1	23.5
$2\sigma_u$	–13.3	–12.5	18.8	–14.1	–13.4	18.7
$3\sigma_g$	–10.3	–10.6	15.6	–12.4	–11.9	16.4
$1\pi_u$	–11.6	–12.4	17.0	–7.2	–7.0	11.4
$1\pi_g$	–1.9	–2.6		–0.3	–0.3	

has a slightly greater atomic number than carbon ($Z=7$ vs $Z=6$), and the nitrogen bond length is somewhat shorter than the carbon-carbon bond (0.110 nm vs 0.120 nm; for reference, the carbon-hydrogen bond length is 0.109 nm). Pairs of molecular orbitals derived from the same atomic orbitals should be deeper on the average in nitrogen and more strongly split. This is born out in the eigenvalues, with the sole exception that the $3\sigma_g$ level is deeper in acetylene than in nitrogen. Oddly, the $3\sigma_g$ eigenvalue would be lower in nitrogen if the N-N distance were larger. Thus, whereas nitrogen is primarily π bonded, the σ component in acetylene is more important. This view is born out by vibrationally resolved studies of the relevant atomic states.³³

The experimental ionization potentials are also given in Table I. The ionization potentials differ from the eigenvalues by a few electron volts which is characteristic of local-density eigenvalues in general. We interpret the region of the calculated continuum with photon energies between the calculated eigenvalue and the experimental ionization potential as being a continuum representation of the "missing" Rydberg states. Thus we believe that *photon energy* not *electron kinetic energy* is the appropriate variable to use for comparison between theory and experiment. This view is supported by the existence of sum rules on the photon energy.^{1,4,51} Moreover, it may be shown that in the present theory, the partial cross sections are zero at threshold, whereas in the presence of a Coulomb potential the partial cross sections are finite at threshold.⁴ The energy range between the eigenvalue and the ionization potential gives the calculation a chance to build up and meet the data at threshold. On the other hand, the theory is incapable of predicting the ionization potential; the neglect of the Coulomb potential in the final state prevents the theory from making a meaningful prediction of the photon energy at threshold.

The optical-frequency polarizabilities for nitrogen and acetylene are shown in Table II. The inclusion of dielectric effects substantially reduces the polarizabilities obtained from the independent-particle approximation, and brings agreement with the data at the level of a few percent. The data of Table II are similar to the result obtained in the TDLDA theory for atoms.¹⁻⁴ The substantial reduction of polarizability has an obvious physical origin; in the static limit, the charge induced by the external field screens the field, so a smaller total moment is induced. In addition to seeking the agreement in the polarizabilities for its own sake, our theory satisfies the sum rule^{14,51}

$$\int_0^\infty \frac{\sigma(\omega)}{\omega^2} d\omega = \frac{2\pi^2}{c} \alpha(0),$$

where $\alpha(0)$ is given by the theory, be it the IPA or the TDLDA. Such a rule is only useful if (as in the case of the TDLDA but not the IPA) the value of $\alpha(0)$ is given approximately correctly. The dispersion from optical frequency to the static limit is small. The IPA and the TDLDA also satisfy the f -sum rule.

TABLE II. Optical-frequency polarizabilities of N_2 and C_2H_2 at 2.71 eV (in cubic angstroms) are given for light polarization parallel (\parallel) and perpendicular (\perp) to the molecular axis.

	α_{\parallel} (\AA^3)	α_{\perp} (\AA^3)
N_2		
IPA	5.10	2.35
TDLDA	2.19	1.55
Expt. (Ref. 34)	2.27	1.55
C_2H_2		
IPA	27.30	4.24
TDLDA	5.46	3.04
Expt. (Ref. 34)	4.86	2.94

B. Partial cross sections

In atomic studies,^{1,4,7} it has been established that if there is a great deal of oscillator strength in a small region of photon energy (be it in a bound-to-bound transition or bound-to-continuum transition) in the IPA, the inclusion of dielectric effects shifts the oscillator strength to higher energies and broadens it. Typically, agreement with experimental data is much improved. On the other hand, when the IPA cross section is featureless, the dielectric screening is of little importance. The same is true in molecules.

It is useful to review the dipole selection rules for the $D_{\infty h}$ group. Parity is always changed, i.e., $g \leftrightarrow u$. For light aligned parallel to the molecular axis, m is unchanged. For light aligned perpendicular to the molecular axis, m is changed by 1, thus $\sigma \leftrightarrow \pi$ and $\pi \leftrightarrow \delta$ are allowed. The gas-phase average is one-third parallel and two-thirds perpendicular light.

The $3\sigma_g$ partial photoemission cross section of nitrogen is shown in Fig. 1(a). The independent-particle cross section shows the "shape resonance" previously identified^{48,49} with the $3\sigma_g \rightarrow \epsilon\sigma_u$ transition. The shape resonance is a final-state effect which may be viewed either as an antibonding combination of atomic p_z orbitals (σ^*) or as a quasibound $l=3$ (about the molecular center) state trapped in the well of the nuclei and prevented from leaking to infinity by the centrifugal barrier for larger radii. In analogy with the studies of rare-gas photoemission, the effect of the TDLDA is to shift the cross section to higher energies, and to broaden it. The agreement with the data is quite striking. The redistribution of oscillator strength is negligible for light perpendicular to the molecular axis. The perpendicular light contribution amounts to a featureless, nearly constant background of 3 Mb over the range of interest.

The calculated cross section for the $3\sigma_g$ level in acetylene, shown in Fig. 1(b), is very similar to the case of nitrogen. The parallel light part of the cross section has structure similar to the shape resonance in nitrogen; the narrow IPA result is shifted and broadened by the introduction of dielectric effects. For light in the perpendicular direction, the featureless cross section of about 3 Mb is

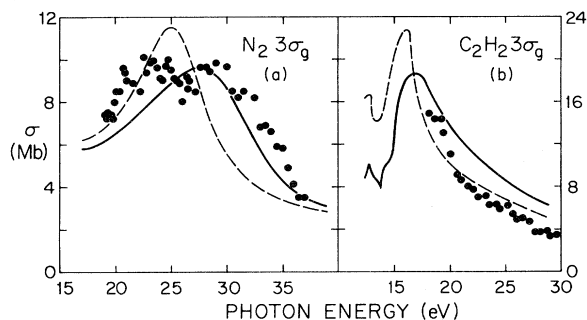


FIG. 1. Partial photoemission cross sections for the $3\sigma_g$ levels of (a) nitrogen and (b) acetylene; theory (---) IPA, (—) TDLDA; experimental data from (a) Ref. 27 and (b) Ref. 36.

little changed by the introduction of dielectric effects. (The exception, a sharp feature around 14 eV, due to the autoionization resonance, is discussed below in the context of $1\pi_u$ level photoemission.) Unfortunately, the agreement with the data is not so good in this case. Semiquantitative agreement is achieved, but the dielectric effects reduce the agreement in this case. The origin of the discrepancy is unclear. Nevertheless, one may regard the $3\sigma_g$ partial cross section as being dominated by a shape resonance, only part of which occurs above the ionization potential in the region accessible to photoemission experiments.

The measured photoemission partial cross sections of the $1\pi_u$ levels in nitrogen and acetylene bear little resemblance to each other, as a comparison of Figs. 2(a) and 2(b) indicates. However, the nitrogen cross section does resemble the *background* of the acetylene cross section. Apart from the resonance in acetylene, the IPA gives a good account of these levels; the broad agreement with experiment is little effected by the introduction of dielectric effects.

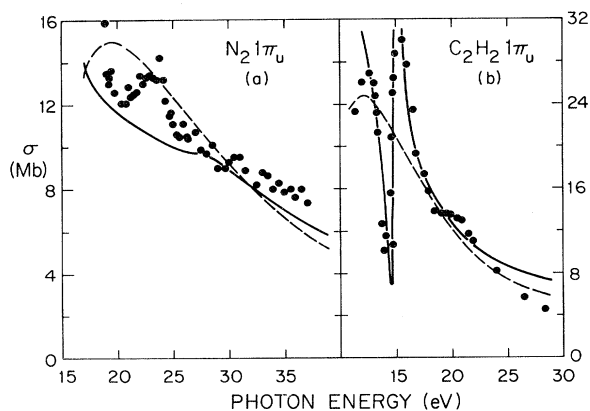


FIG. 2. Partial photoemission cross sections for the $1\pi_u$ levels of (a) nitrogen and (b) acetylene; theory (---) IPA, (—) TDLDA; experimental data from (a) Ref. 27 and (b) Ref. 36.

The resonance in the $1\pi_u$ level in acetylene is primarily the result of a Fano autoionization.⁸ The $2\sigma_u \rightarrow 1\pi_g$ transition is predicted to occur at 13.1 eV in the single-center calculation, and 13.8 eV in the Gaussian-orbital calculation. Since this energy is above the ionization potential for the $1\pi_u$ electrons, this bound-to-bound transition strongly influences the self-consistent field as the photon energy is varied through this region. Indeed, the independent-particle susceptibility has a pole for photon energy equal to the eigenvalue difference of an occupied and an unoccupied bound state. In view of this, the presence of a sharp structure in the cross section is reasonable. The calculated $3\sigma_g$ cross section in acetylene is similarly effected, but the energy in question is below the ionization potential for this level rendering the feature unobservable by photoemission. No autoionization is predicted for nitrogen simply because there is no symmetry-allowed bound-to-bound transition with an energy greater than the eigenvalue of some other level. The autoionization resonances in nitrogen involving the Rydberg series^{26,27} do not appear because the Rydberg states are smeared to a continuum in the neutral potential of our calculation.

The autoionization resonance is not sufficient to account for all of the cross section very near threshold. However, a second mechanism may be observed in the calculation. For light parallel to the molecular axis, the IPA predicts a very small cross section for the $1\pi_u$ level in both nitrogen and acetylene. The *f*-sum rule is satisfied almost completely by oscillator strength associated with the discrete $1\pi_u \rightarrow 1\pi_g$ (or $\pi \rightarrow \pi^*$) transition.^{36,52} The TDLDA readjusts this oscillator strength, adding a piece to the calculated continuum. In acetylene, some of this appears above the physical threshold to account for the missing cross section. In nitrogen, the same mechanism is active, but only the part of the continuum between the eigenvalue and the ionization potential is effected; thus the effect is unobservable by photoemission. This effect is in strict analogy to the physics of atomic barium,⁷ the only difference being that in barium the oscillator strength is pushed farther into the observable region.

A minor but well-established feature of the photoemission spectra in nitrogen is the two-electron excitation^{26,27} in the region of photon energies from about 22 to 25 eV. A virtual state is formed in which the $1\pi_g$ and a Rydberg state are occupied. The rapid decay of one of these electrons into a core hole ejects the other into the continuum. The process has a non-negligible strength presumably because the $1\pi_u \rightarrow 1\pi_g$ transition has great oscillator strength. Since the present theory only accounts for single-particle excitations such a feature would not be expected to be seen in the present calculation. Indeed it is not. There are similar small features in the cross sections of all levels considered so far which are not accounted for by the present theory; these are in the vicinity of 22 to 25 eV for nitrogen and 18 to 22 eV in acetylene. It seems probable that these features are associated with the same two-electron excitation in acetylene as in nitrogen. With this interpretation, the modest difference in energies is due to the difference in the $1\pi_u \rightarrow 1\pi_g$ transition energies which are 9.7 eV for nitrogen and 6.9 eV for acetylene in our Gaussian-orbital calculation. That is, if there were no

other differences between nitrogen and acetylene, the two-electron excitation would be expected to lie about 3 eV lower in acetylene than in nitrogen.

C. Angular distributions

Additional information about gas-phase photoemission spectra may be obtained from the asymmetry parameter $\beta(\omega)$. As noted above, β is related to the angular distribution of the outgoing electrons; $\sigma(\omega)$ and $\beta(\omega)$ together form all the information obtainable from a nonchiral gas-phase target in the electric dipole approximation.¹³ Overall, there is good agreement between the theoretical and experimental β values.

The most striking feature occurs in the $1\pi_u$ level of acetylene, shown in Fig. 3 of Ref. 9. The experimental data^{38,39} show a general increase in the range of photon energies from 13 to 26 eV with the exception of a large dip in the range 13–17 eV. The present independent-particle calculation does not reproduce the dip in the spectrum, only the background. The inclusion of dielectric effects, on the other hand, produces a prominent dip in rough quantitative agreement with experiment. The general picture of an autoionization resonance in this spectral region is reinforced by the existence, and explanation, of this feature.

In the $3\sigma_g$ level of acetylene, the TDLDA predicts a dip in β which is similar to the $1\pi_u$ level calculation in location and magnitude.⁵⁰ This structure is only of theoretical interest, since the photon energies in question are below the physical ionization threshold. Above threshold, the TDLDA brings about a marked improvement in the agreement with experiment compared to the independent-particle calculation. It is somewhat curious that the introduction of dynamic screening should improve agreement with β but reduce the agreement with σ for this level.

In nitrogen, good agreement with the experimental data³⁰ is achieved for both the $3\sigma_g$ level and the $1\pi_u$. For these levels, the effect of dielectric screening improves the agreement with experiment marginally at best. The discontinuity in the experimental asymmetry data shown in Fig. 3 around 23 eV may be related to the two-electron

state discussed above. The evidence for this is the energy is the same and the calculations do not reproduce the feature. If two-electron effects were important in this spectral region, we would expect to see them in both levels of both molecules. In the experimental nitrogen $1\pi_u$ and acetylene $3\sigma_g$ spectra, the data is ambiguous. For acetylene $1\pi_u$, structure in β does appear at about the same energy as the hypothesized two-electron excitation in the cross section.

D. Comparison with other calculations

Photoemission from nitrogen and acetylene have been studied before using a variety of techniques. Hartree-Fock based approaches include Stieltjes-Tchebycheff moment analysis^{12,36,44,45,52} and the Schwinger variational principle applied using a single-center expansion.⁴⁷ Additionally, the $X\alpha$ scattered-wave ($X\alpha$ SW) method had been applied.^{39,48,49} The Stieltjes-Tchebycheff theory has been extended to the time-dependent Hartree-Fock level in a study of nitrogen photoemission with light aligned along the molecular axis only.¹²

To a certain extent, the previous calculations were of similar quality to the present ones; however, there are some important exceptions. First, the autoionization resonance in the $1\pi_u$ level of acetylene is not accounted for by Hartree-Fock theory in a calculation of the cross sections,³⁷ or by the $X\alpha$ SW approximation for the asymmetry parameter³⁹ (these being the only available studies). The background of these curves is more or less correctly given; these calculations are comparable to the present IPA. Second, the Hartree-Fock calculation of the $1\pi_u$ photoemission cross section in nitrogen is much too large.^{12,47} The $1\pi_u \rightarrow 1\pi_g$ transition appears in the continuum. A random-phase approximation with exchange (RPAE) calculation¹² or special procedures⁴⁷ are necessary to push the spurious oscillator strength below the photoemission threshold. Third, there are indications that there are non-Franck-Condon effects in the $3\sigma_g$ level of molecular nitrogen.⁵³ This may limit the extent to which the present fixed nuclei calculation can explain certain details of the photoemission cross section and asymmetry parameter.

It is worth noting that the $X\alpha$ SW calculation of the $3\sigma_g$ level in nitrogen is in better agreement with the present IPA calculation than a cursory glance at the published figures would indicate. While Davenport⁴⁹ reports a peak at 32 eV, his curve has been shifted by 7 eV to adjust the calculated threshold (i.e., the $3\sigma_g$ eigenvalue) to the experimental ionization potential. If this shift is omitted, the $X\alpha$ SW peak is at 25 eV, which is the same as the present IPA calculation. The peak heights and widths remain somewhat different, however.

IV. CONCLUSIONS

The TDLDA has been extended to allow the treatment of dynamical screening or "dielectric effects" in the photoresponse of molecules using a single-center expansion. The single-center expansion has been used extensively by other authors in the study of molecular photoemission and

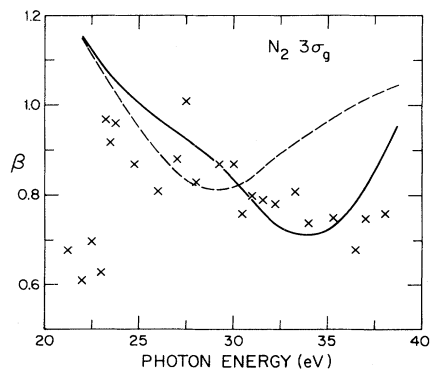


FIG. 3. Gas-phase photoemission asymmetry parameter for the $3\sigma_g$ level of nitrogen; theory (— — —) IPA, (—) TDLDA; experimental data from Ref. 30.

electron scattering. On the other hand, studies of molecular photoresponse at the present level (equivalent to the RPAAE) are very few. The present theory is capable of predicting static and optical-frequency polarizabilities, photoemission cross sections, and asymmetry parameters, and may be extended to the problem of hyperpolarizabilities and multiphoton ionization as well.

The inclusion of dielectric effects causes a marked reduction in the calculated values of the optical-frequency polarizability yielding agreement with experiments. As suggested by general theoretical arguments and atomic TDLDA calculations, the inclusion of dielectric effects shifts oscillator strength to higher energies. In the present systems, this effect is somewhat subtle; the inclusion of these effects improves agreement with experiment only in certain cases. It would have been difficult to appreciate the importance of this shift in the context of a model potential (e.g., a muffin-tin potential): One could always imagine that the difference between the independent-particle calculation and the experiment was due to an inaccurate description of the potential. In acetylene, an autoionization resonance in the $1\pi_u$ level is calculated yielding agreement with experiment in both the photoemission partial cross section and the asymmetry parameter.

ACKNOWLEDGMENTS

We wish to thank R. P. Messmer for allowing us to use the Gaussian-orbital program. We are grateful to A. Zangwill for many useful discussions. This work was supported by the Gas Research Institute and by the National Science Foundation Materials Research Laboratories Program under Grant No. DMR-79-23647.

APPENDIX

Our purpose in this appendix is to present the constructive procedure used for computing the Green's function in a single-center representation. A similar procedure has been presented by Nesbet.⁵⁴ The Green's function satisfies the equation

$$(\omega - H_r)G(\vec{r}, \vec{r}') = \delta(\vec{r} - \vec{r}') , \quad (\text{A1})$$

and a similar equation in r' . As discussed in the text, we expand $G(\vec{r}, \vec{r}')$ in spherical harmonics in both variables

$$G(\vec{r}, \vec{r}') = \sum_{L, L'} Y_L(\Omega) G_{LL'}(r, r') Y_{L'}(\Omega') , \quad (\text{A2})$$

where in principle the double summation runs over all values of $L \equiv (l, m)$ and in practice the summations are truncated as described in the text. Substitution into (A1) leads to

$$(E + \nabla_l^2) G_{LL'}(r, r') - \sum_{L_1} V_{LL_1}(r) G_{L_1 L'}(r, r') = \frac{\delta_{LL'} \delta(r - r')}{rr'} ,$$

where the quantities $V_{LL'}$ are defined in Eq. (9) and the right-hand side arises from the relation

$$\delta(\vec{r} - \vec{r}') = \sum_L Y_L(\Omega) Y_L(\Omega') \frac{\delta(r - r')}{rr'} .$$

The angular components of the Green's function satisfy the coupled-channel differential equations (10) in both arguments. Regarded as a function of r , at the point $r = r'$ the angular components must be continuous in value and have the proper discontinuity in slope to produce the δ function in the second derivative. The first condition implies that

$$G_{LL'}(r, r') \big|_{r=r'+0} = G_{LL'}(r, r') \big|_{r=r'-0} , \quad (\text{A3})$$

while the second condition implies

$$r^2 \left[\frac{d}{dr} G_{LL'}(r, r') \big|_{r=r'+0} - \frac{d}{dr} G_{LL'}(r, r') \big|_{r=r'-0} \right] = \delta_{LL'} . \quad (\text{A4})$$

Our method for constructing the Green's function is as follows. We integrate the coupled-channel equations starting at the origin of coordinates to find N independent solutions, where, as was discussed in the text, N denotes the number of symmetry-allowed (l, m) components within the restricted angular momentum subspace. We use a matrix Numerov method and include the stabilization procedure discussed in Refs. 50 and 54. We find the K matrix in the standard way and diagonalize it to find the eigenphase shifts and then the regular eigenchannel solutions. The form of the eigenchannel solutions depends upon whether the energy is positive or negative. For positive energies, with $k^2 = E$, the eigenchannel solutions have the asymptotic form

$$\psi_n(\vec{r}) \rightarrow (1 + \lambda_n^2)^{-1/2} \sum_L [j_l(kr) - \lambda_n n_l(kr)] Y_L(\Omega) C_{Ln} , \quad (\text{A5})$$

where the quantities λ_n and C_{Ln} are the eigenvalues and eigenvectors of the K matrix

$$\sum_{L'} K_{LL'} C_{L'n} = \lambda_n C_{Ln} .$$

(These eigenvalues are often parametrized in terms of phase shifts δ_n with the relationship $\lambda_n = -\tan \delta_n$.) Using a sequence of matrix manipulations, the regular eigenchannel solutions at points where the potential is vanishing is easily found in terms of the initial set of regular solutions. For general values of r the regular eigenchannel solutions will be written in the form

$$\psi_n(\vec{r}) = \sum_L \psi_{Ln}(r) Y_L(\Omega) .$$

We also need eigenchannel solutions for negative energies. Let i_l and k_l be the modified spherical Bessel and Hankel functions, respectively, which are defined by the relations

$$i_l(kr) = i^{-1} j_l(ikr)$$

and

$$k_l(kr) = i^l [j_l(ikr) + in_l(ikr)],$$

where in this regime $k^2 = -E$. A K matrix may be defined by forming regular solutions having the asymptotic form

$$\sum_L \left[i_l(kr) Y_L(\Omega) - \sum_{L'} K_{LL'} k_{L'}(kr) Y_{L'}(\Omega) \right].$$

The K matrix is still real and symmetric and diagonalization allows one to form eigenchannel solutions according to the definition

$$\psi_n \rightarrow \sum_L [i_l(kr) - \lambda_n k_l(kr)] Y_L(\Omega) C_{Ln}.$$

Every regular eigenchannel solution $\psi_n(\vec{r})$ has a corresponding irregular solution ξ_n . For positive energies the irregular solution is defined to have the asymptotic form

$$\xi_n(\vec{r}) \rightarrow (1 + \lambda_n^2)^{1/2} \sum_L [n_l(kr) + \lambda_n j_l(kr)] Y_L(\Omega) C_{Ln}, \quad (\text{A6})$$

while for negative energies

$$\xi_n(\vec{r}) \rightarrow \sum_L k_l(kr) Y_L(\Omega) C_{Ln}.$$

These forms, of course, hold only in the asymptotic region where the potential vanishes. For smaller values of r we integrate inwards using (A6) to supply the initial conditions. For arbitrary r the irregular eigenchannel solutions will be written as

$$\xi_n(\vec{r}) = \sum_L \xi_{Ln}(r) Y_L(\Omega).$$

Together the set (A5) and (A6) span the restricted angular momentum subspace.

Since the Green's-function components satisfy the coupled-channel equations they can be written as some bilinear combination of any complete set of solutions. A representation of this type takes a particular concise form when the complete set employed are the (regular and irregular) eigenchannel solutions. We show below that for positive energies the angular momentum components of the Green's function defined by (A2) may be expressed in the form

$$G_{LL'}(r, r') = \begin{cases} \sum_n k \psi_{Ln}(r) [\xi_{L'n}(r') - i \psi_{L'n}(r')], & r < r' \\ \sum_n k [\xi_{Ln}(r) - i \psi_{Ln}(r)] \psi_{L'n}(r'), & r > r' \end{cases} \quad (\text{A7})$$

while for negative energies

$$G_{LL'}(r, r') = \begin{cases} \sum_n k \psi_{Ln}(r) \xi_{L'n}(r'), & r < r' \\ \sum_n k \xi_{Ln}(r) \psi_{L'n}(r'), & r > r'. \end{cases} \quad (\text{A8})$$

It is clear from inspection of the asymptotic forms of the eigenchannel solutions that the quantities just defined satisfy the boundary conditions at infinity, outgoing wave

for positive energies and decaying for negative energies. For positive energies, the outgoing wave boundary conditions are required by the sign of the infinitesimal in the spectral sum (4). The forms (A7) and (A8) satisfy the conditions (A3) and (A4) provided that

$$\sum_n [\xi_{Ln}(r) \psi_{L'n}(r) - \psi_{Ln}(r) \xi_{L'n}(r)] = 0 \quad (\text{A9})$$

and

$$\sum_n [\xi'_{Ln}(r) \psi_{L'n}(r) - \psi'_{Ln}(r) \xi_{L'n}(r)] = \frac{\delta_{LL'}}{kr^2}, \quad (\text{A10})$$

where the primes denote differentiation with respect to r .

In order to verify (A9) and (A10) we develop some general relations between regular and irregular solutions to the coupled-channel equations. Let the sets of functions $\{F_L(r)\}$ and $\{G_L(r)\}$ represent any two solution vectors. Then direct substitution into the differential equations shows that the Wronskian

$$W(F, G) \equiv r^2 \sum_L [F_L(r) G'_L(r) - F'_L(r) G_L(r)]$$

is a constant. Using the asymptotic forms (A5) and (A6) and the orthonormality of the eigenvectors of the K matrix, it follows that

$$W(\psi_n, \psi_m) = W(\xi_n, \xi_m) = 0$$

while

$$W(\psi_n, \xi_m) = \frac{1}{k} \delta_{nm}.$$

Now let $J_n(\vec{r})$ denote any N linearly independent regular solutions to the coupled-channel equations which satisfy the Wronskian relations

$$W(J_n, J_m) = 0. \quad (\text{A11})$$

We form the matrix $\mathcal{J}(r)$ whose n th column is the solution vector $J_{Ln}(r)$. The linear independence of the N solutions ensures that the matrix is nonsingular. Define the matrix P

$$P_{nm}(r) = \int_{\alpha}^r \{[\mathcal{J}^\dagger(r') \mathcal{J}(r')]^{-1}\}_{nm} (r')^{-2} dr', \quad (\text{A12})$$

where the lower integration limit is an arbitrary constant. We define the quantities

$$N_{Lm}(r) = \sum_n J_{Ln}(r) P_{nm}(r). \quad (\text{A13})$$

Straightforward differentiation and use of the Wronskian relations (A11) shows that these satisfy the relations

$$\frac{dN_{Lm}}{dr} = \sum_n \frac{dJ_{Ln}}{dr} P_{nm} + \frac{1}{r^2} [(\mathcal{J}^\dagger)^{-1}]_{Lm}$$

and

$$\nabla_l^2 N_{Lm} = \sum_n (\nabla_l^2 J_{Ln}) P_{nm}(r).$$

These relations may be used to show that the functions

$$N_m(\vec{r}) = \sum_n N_{Lm}(r) Y_L(\Omega)$$

are solutions to the coupled-channel equations which satisfy the Wronskian relations

$$W(J_n, N_m) = \delta_{nm}.$$

Furthermore, the J_n and the N_m are linearly independent. This procedure whereby one can generate N additional solutions given knowledge of the set $J_n(\vec{r})$ is a direct generalization of the procedure discussed in, e.g., Morse and Feshbach⁵⁶ for generating a second solution to a one-dimensional second-order differential equation.

Now replace the set J_n by the regular eigenchannel solutions ψ_n . Since the ψ_n and the set generated by Eq. (A13) (with J_n replaced by ψ_n) form $2N$ linearly independent solutions, then for some choice of constants A_{nm} and B_{nm}

$$\xi_n = \sum_m (A_{nm} \psi_m + B_{nm} N_m).$$

But use of the Wronskian relations among the ψ_n and ξ_m shows that $B_{nm} = k^{-1} \delta_{nm}$ while use of the Wronskians among the ξ_n shows that A_{nm} must be symmetric. Thus

$$\xi_{Lm}(r) = k^{-1} \sum_n \psi_{Ln}(r) Q_{nm}(r), \quad (\text{A14})$$

where the matrix Q differs from P by a constant symmetric matrix. The proof of the relations (A9) and (A10) is now immediate. Substitution of (A14) into (A9) shows that the latter is true, owing to the symmetry of Q . The differentiation required by the substitution of Eq. (A14) into (A10) may be carried out using the definition of P in Eq. (A12).

*Present address: Western Electric Engineering Research Center, P.O. Box 900, Princeton, NJ 08540.

¹A. Zangwill and P. Soven, Phys. Rev. A **21**, 1561 (1980).

²M. J. Scott and E. Zaremba, Phys. Rev. A **21**, 12 (1980); **22**, 2293(E) (1980).

³G. D. Mahan, Phys. Rev. A **22**, 1780 (1980).

⁴A. Zangwill, Ph.D. thesis, University of Pennsylvania, 1981.

⁵A. Zangwill, J. Chem. Phys. **78**, 5926 (1983).

⁶J. L. Dehmer, A. F. Starace, U. Fano, J. Sugar, and J. W. Cooper, Phys. Rev. Lett. **26**, 1521 (1971).

⁷A. Zangwill and P. Soven, Phys. Rev. Lett. **45**, 204 (1980).

⁸U. Fano, Phys. Rev. **124**, 1866 (1961).

⁹Z. Levine and P. Soven, Phys. Rev. Lett. **50**, 2074 (1983).

¹⁰P. A. M. Dirac, Proc. Camb. Philos. Soc. **26**, 376 (1930).

¹¹D. Pines and P. Nozières, *The Theory of Quantum Liquids* (Benjamin, New York, 1966).

¹²G. R. J. Williams and P. W. Langhoff, Chem. Phys. Lett. **78**, 21 (1981).

¹³B. Ritchie, Phys. Rev. A **13**, 1141 (1975); **14**, 359 (1975).

¹⁴J. C. Tully, R. S. Berry, and B. J. Dalton, Phys. Rev. **176**, 95 (1968).

¹⁵J. L. Dehmer, D. Dill, and A. C. Parr, in *Photophysics and Photochemistry in the Vacuum Ultraviolet*, edited by S. McGlynn, G. Findley, and R. Huebner (Reidel, Dordrecht, Holland, 1983).

¹⁶J. C. Slater, Phys. Rev. **81**, 385 (1951); P. Hohenberg and W. Kohn, *ibid.* **136**, B864 (1964); W. Kohn and L. J. Sham, *ibid.* **140**, A1133 (1965).

¹⁷L. Hedin and B. I. Lundqvist, J. Phys. C **4**, 2064 (1971).

¹⁸B. I. Dunlop, J. W. D. Connolly, and J. R. Sabin, J. Chem. Phys. **71**, 3396 (1979); **71**, 4993 (1979).

¹⁹F. B. van Duijneveldt, IBM Research Laboratory Report No. RJ945-16437, 1971 (unpublished).

²⁰K. Schwarz, Phys. Rev. B **5**, 2466 (1972).

²¹R. G. Gordon, J. Chem. Phys. **51**, 14 (1969).

²²D. Loomba, S. Wallace, D. Dill, and J. L. Dehmer, J. Chem. Phys. **75**, 4549 (1981).

²³F. S. Acton, *Numerical Methods That Work* (Harper & Row, New York, 1970); called "Shank's method" in C. M. Bender and S. A. Orszag, *Advanced Mathematical Methods for Scientists and Engineers* (McGraw-Hill, New York, 1978).

²⁴G. Breit and H. A. Bethe, Phys. Rev. **93**, 888 (1954).

²⁵L. C. Lee, R. W. Carlson, D. L. Judge, and M. Ogawa, J. Quant. Spectrosc. Radiat. Transfer **13**, 1023 (1973).

²⁶E. W. Plummer, T. Gustafsson, W. Gudat, and D. E. Eastman, Phys. Rev. A **15**, 2339 (1977).

²⁷P. R. Woodruff and G. V. Marr, Proc. R. Soc. London Ser. A **358**, 87 (1977).

²⁸A. Hamnett, W. Stoll, and C. E. Brion, J. Electron Spectrosc. Relat. Phenom. **8**, 357 (1976).

²⁹G. R. Wight, M. J. Van der Wiel, and C. E. Brion, J. Phys. B **9**, 675 (1976).

³⁰G. V. Marr, J. M. Morton, R. M. Holmes, and D. G. McKoy, J. Phys. B **12**, 43 (1979).

³¹R. M. Holmes and G. V. Marr, J. Phys. B **13**, 945 (1980).

³²J. Kriele and A. Schweig, J. Electron Spectrosc. Relat. Phenom. **20**, 191 (1980).

³³W. C. Price, in *Advances in Atomic and Molecular Physics*, edited by D. R. Bates and B. Bederson (Academic, New York, 1974), Vol. 10, p. 131.

³⁴G. R. Alms, A. K. Burnham, and W. Flygare, J. Chem. Phys. **63**, 3321 (1975).

³⁵R. Unwin, I. Khan, N. V. Richardson, and A. M. Bradshaw, Chem. Phys. Lett. **77**, 242 (1981).

³⁶P. W. Langhoff, B. V. McKoy, R. Unwin, and A. M. Bradshaw, Chem. Phys. Lett. **83**, 270 (1981).

³⁷J. Kreile, A. Schweig, and W. Thiel, Chem. Phys. Lett. **79**, 547 (1981).

³⁸A. C. Parr, D. L. Ederer, J. B. West, D. M. P. Holland, and J. L. Dehmer, J. Chem. Phys. **76**, 4349 (1982).

³⁹P. R. Keller, D. Mehaffy, J. W. Taylor, F. A. Grimm, and T. A. Carlson, J. Electron. Spectrosc. Relat. Phenom. **27**, 233 (1982).

⁴⁰*Electron-Molecule and Photon-Molecule Collisions*, edited by T. N. Rescigno, V. McKoy, and B. Scheider (Plenum, New York, 1979).

⁴¹G. Raseev, H. LeRouzo, and H. Lefebvre-Brion, J. Chem. Phys. **72**, 5701 (1980).

⁴²W. D. Robb and L. A. Collins, Phys. Rev. A **22**, 2474 (1980).

⁴³L. A. Collins, W. D. Robb, and M. A. Morrison, J. Phys. B **12**, L777 (1978); Phys. Rev. A **21**, 488 (1980).

⁴⁴T. N. Rescigno and P. W. Langhoff, Chem. Phys. Lett. **51**, 65

- (1977).
- ⁴⁵T. N. Rescigno, A. Gerwer, B. V. McKoy, and P. W. Langhoff, *Chem. Phys. Lett.* **66**, 116 (1979).
- ⁴⁶T. N. Rescigno, C. F. Bender, B. V. McKoy, and P. W. Langhoff, *J. Chem. Phys.* **68**, 970 (1978).
- ⁴⁷R. R. Lucchese, G. Raseev, and V. McKoy, *Phys. Rev. A* **25**, 2572 (1982).
- ⁴⁸J. L. Dehmer and D. Dill, *Phys. Rev. Lett.* **35**, 213 (1975).
- ⁴⁹J. W. Davenport, *Phys. Rev. Lett.* **36**, 945 (1976).
- ⁵⁰Z. H. Levine, Ph.D. thesis, University of Pennsylvania, 1983.
- ⁵¹U. Fano and J. W. Cooper, *Rev. Mod. Phys.* **40**, 441 (1968), Sec. 2.5.
- ⁵²L. E. Mechado, E. P. Leal, C. Csanak, B. V. McKoy, and P. W. Langhoff, *J. Electron. Spectrosc. Relat. Phenom.* **25**, 1 (1982).
- ⁵³J. B. West, A. C. Parr, B. E. Cole, D. L. Ederer, R. Stockbauer, and J. L. Dehmer, *J. Phys. B* **13**, L105 (1980); J. L. Dehmer, D. Dill, and S. Wallace, *Phys. Rev. Lett.* **43**, 1005 (1979); G. Raseev, H. LeRouzo, and H. Lefevbre-Brion, *J. Chem. Phys.* **72**, 5701 (1980); R. R. Lucchese and B. V. McKoy, *J. Phys. B* **14**, L629 (1981).
- ⁵⁴Robert K. Nesbet, *Variational Methods in Electron-Atom Scattering Theory* (Plenum, New York, 1980), Sec. 2.7.
- ⁵⁵Z. H. Levine (unpublished).
- ⁵⁶P. M. Morse and H. Feshbach, *Methods of Theoretical Physics* (McGraw-Hill, New York, 1953), p. 525.